Asian Journal of Information Technology 7 (8): 344-349, 2008
ISSN: 1682-3915

Dispersion and Confinement Loss of Photonic Crystal Fiber

M. Jalal Uddin and M. Shah Alam
Department of Electrical and Electronic Engineering,
Bangladesh University of Engineering and Technology, Dhaka-1000, Bangladesh

Abstract: A detailed modal analysis of Photonic Crystal Fiber (PCF) is carried out by using the Finite Element Method (FEM) in FEMLAB environment. The effective mode index of the fundamental mode is found out for different PCF structures and the effective mode area is calculated for varying number of air hole rings. Finally, dispersion and confinement loss properties of different PCF structures are numerically calculated and it is found that the dispersion and confinement loss profile of the PCF can be controlled by appropriately choosing diameter, pitch and number of air hole rings. The results show that the effective mode area and the confinement loss decreases with the increase in number of air hole rings and the dispersion increases with the increase in number of air hole rings.

Key words: Photonic Crystal Fiber (PCF), dispersion, confinement loss, Finite Element Method (FEM)

INTRODUCTION

Broadband optical transmission with wavelength division multiplexing technique is effective for large capacity networks and optical fibers are widely used as optical transmission media. However, chromatic and modal dispersion, nonlinearity and losses restrict the wavelength region available for these fibers.

Photonic Crystal Fibers (PCFs) recently attracted a great deal of interest because of their excellent propagation properties (Russel, 2003; Knight, 2003). Many research groups all over the world are making constant effort to establish the superiority of PCFs over conventional fibers because of its novel optical characteristics. It has been reported that PCF can realize endlessly single-mode operation (Birks *et al*., 1997), flexible chromatic dispersion over a wide wavelength range (Saitoh and Koshiba, 2003; Shen *et al*., 2003; Matsui *et al*., 2005), large effective area (Matsui *et al*., 2005; Knight *et al*., 1998), controllable nonlinearity (Knight *et al*., 1998), ultralow loss (Tajima *et al*., 2004; Finazzi *et al*., 2003) and high group birefringence (Alam *et al*., 2005). Basically, PCFs are single-material fibers with an arrangement of air holes running along the length of the fiber and they provide confinement and guidance of light in a defect region around the centre. As for the light confinement mechanism, index guiding PCFs rely on total internal reflection to confine light in the region of a missing air hole forming a central core.

Various methods have been used for analysis of PCFs (White *et al*., 2002; Ferrando *et al*., 1999) each of which has its advantages and limitations. In this research, the FEM is used to find modal, dispersion and confinement loss characteristics of PCFs in FEMLAB environment. The effect of structural parameters on effective mode index, effective modal area, dispersion and confinement loss properties are studied in detail. The results are compared with the existing published results and found a very good agreement.

MATERIALS AND METHODS

The FEMLAB based finite element technique is used in this work for the analysis of dispersion properties of PCF. Figure 1 shows the transverse cross section of a typical PCF consists of a central high index defect region or a missing hole in a regular triangular or hexagonal array of air holes. There are 3 design parameters: the air hole diameter day, the spacing between holes or pitch Λ and the number of air hole rings N_r.

For practical purpose, it is considered that the surrounding wall of the PCF is Perfect Magnetic Conductor (PMC) that constrains the tangential magnetic field to be zero on their surface. The boundary condition becomes:

$$a_n \times H = 0 \quad (1)$$

Corresponding Author: M. Jalal Uddin, Department of Electrical and Electronic Engineering,
Bangladesh University of Engineering and Technology, Dhaka-1000, Bangladesh

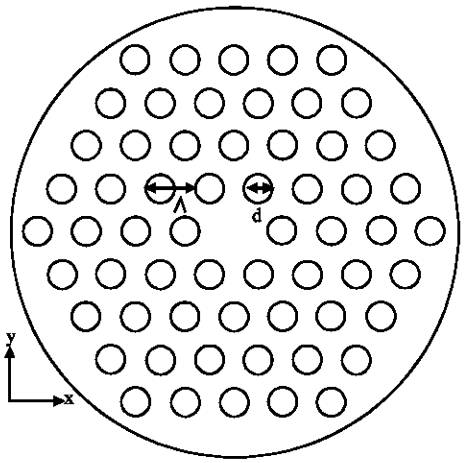

Fig. 1: The cross section of PCF with a regular triangular air hole array defined by the air hole diameter d and the pitch Λ

Here, a_n is the unit normal on the surface. The inner air hole and fiber material should maintain a boundary condition for continuity of field. The boundary condition for the inner boundaries is:

$$a_n \times (H_1 - H_2) = 0 \tag{2}$$

The modal analysis is carried out, first on the cross section in the x-y plane of the fiber, i.e., on the cross section of the fiber as shown in Fig. 1. It is assumed that the wave propagates in the z-direction and has the form,

$$H(x, y, z, t) = H(x, y, z)\exp[j(\omega t - \beta z)] \tag{3}$$

where:

ω = The angular frequency.
β = The propagation constant.

An eigenvalue equation in terms of the magnetic field H is derived from the Helmholtz equation,

$$\nabla \times (n^{-2}\nabla \times H) - k_0^2 H = 0 \tag{4}$$

and is solved for the eigenvalue of $-\beta^2$.

In FEMLAB, however, modal analysis of a perpendicular hybrid-mode wave using electromagnetics module is done. The eigenvalue equation is solved to give effective mode index,

$$n_{eff} = \frac{\beta}{k_0} \tag{5}$$

of a guided mode for a given wavelength. Here, k_0 is the free space wavenumber. Once, the modal solution is obtained, various post-processing data is readily available for visualization of the solution in different ways.

The effective mode index has both real and imaginary parts. The chromatic dispersion of PCF is calculated easily (Saitoh and Koshiba, 2003) from the real part of the effective mode index n_{eff} values versus wavelength using,

$$D(\lambda) = -\frac{\lambda}{c}\frac{d^2}{d\lambda^2}\{\mathrm{Re}[n_{eff}(\lambda)]\} \tag{6}$$

where:

λ = The wavelength.
c = The velocity of light.

In order to check, the accuracy of the results found here, we considered an index guiding PCF with a single core of six equally spaced air holes with hole diameter d = 5 μm, pitch Λ = 6.75 μm, the background refractive index n = 1.45 and the operating wavelength, λ = 1.45 μm. The effective index found here, n_{eff} = 1.445395 + i 1.807358×10^{-19}. This result is in good agreement with that of the full vector FEM (Saitoh and Koshiba, 2003) except that of the imaginary part of the effective mode index. The limitation of finite element method in calculating the imaginary part of the effective index is stated in (Zolla *et al*., 2005). The confinement loss of the photonic crystal fiber can be calculated (Saitoh and Koshiba, 2003) by using the imaginary part of the effective mode index,

$$\text{Confinement loss} = 8.686 \times \mathrm{Im}\,[k_0 n_{eff}]\ \text{dB/m}, \tag{7}$$

where, Im stands for the imaginary part.

Another important property of the fiber, the effective mode area, A_{eff} can be calculated (Saitoh and Koshiba, 2003) using the electric field as,

$$A_{eff} = \frac{\left(\iint |E|^2\,dxdy\right)^2}{\iint |E|^4\,dxdy} \tag{8}$$

The area integration is carried out over the cross section of the fiber and the electric field intensity E is given by,

$$E = \sqrt{E_x^2 + E_y^2} \tag{9}$$

where:

E_x = Is the x-component of the electric field.

E_y = Is the y-component of the electric field.

RESULTS AND DISCUSSION

In Fig. 2, two dimensional surface plots and contour plots for the electric field distribution are presented for different number of air hole rings. It is clear, from the plots that the propagating light becomes more concentrated in the centre, decreasing the spot size when the number of air hole rings is increased.

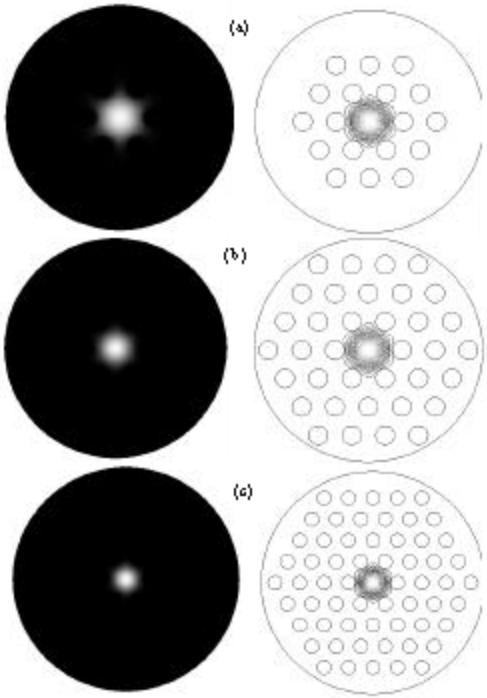

Fig. 2: Two dimensional surface field distribution and contour plot. (a) for 2 air hole ring, (b) for 3 air hole ring and (c) for 4 air hole rings

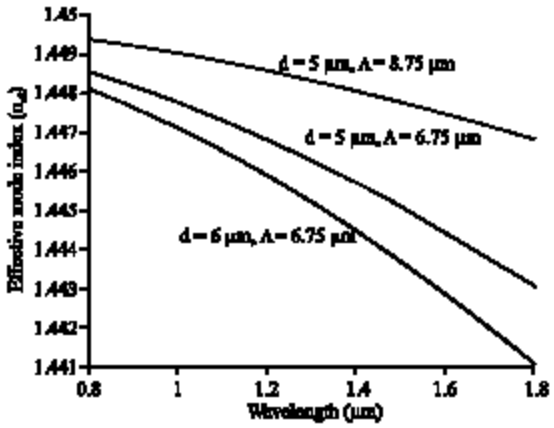

Fig. 3: Effective index as a function of wavelength. The variation of effective index with the air hole diameter, d and pitch, Λ is also shown in the figure. One air hole ring is used in each case

The effective mode index is found out for each operating wavelength and for different PCF structures. Figure 3 shows the plot of effective mode index versus wavelength for different structural parameters. It is found that the effective mode index decreases with the increase in wavelength, which is in good agreement with Matsui *et al*. (2005) and increases with the decrease of air hole diameter and with the increase of pitch.

Figure 4 shows the variation of effective mode area against the number of air hole rings. It is clear that the

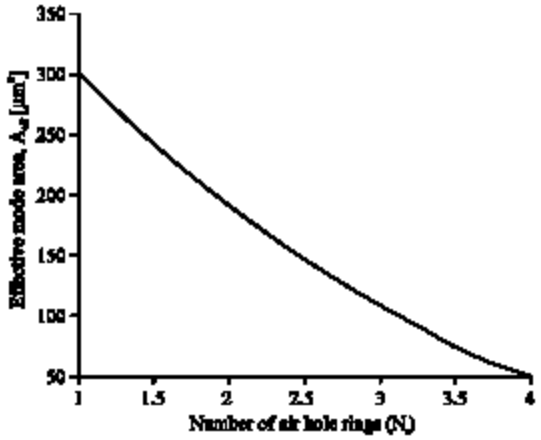

Fig. 4: Effective mode area as a function of number of air hole rings, Nr. Air hole diameter d = 6 μm and pitch Λ = 6.75 μm

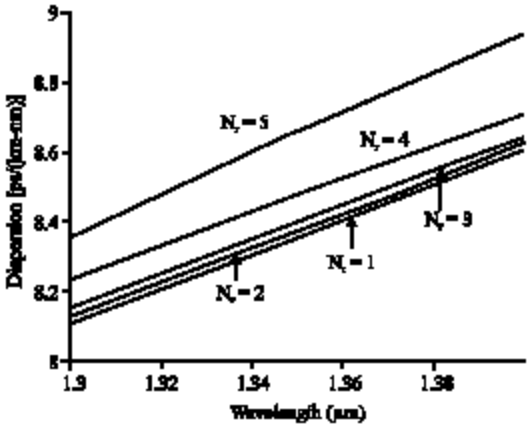

Fig. 5: Dispersion of photonic crystal fiber against wavelength for different number of air hole rings. Air hole diameter, d = 5 μm and hole spacing, Λ = 6.75 μm

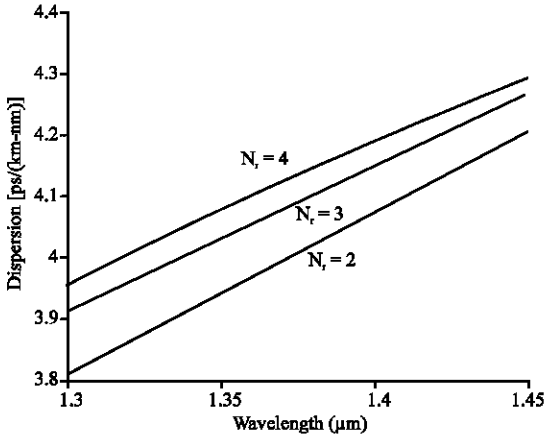

Fig. 6: Dispersion of photonic crystal fiber against wavelength for different number of air hole rings. Air hole diameter, d = 5 μm and hole spacing, Λ = 8.75 μm

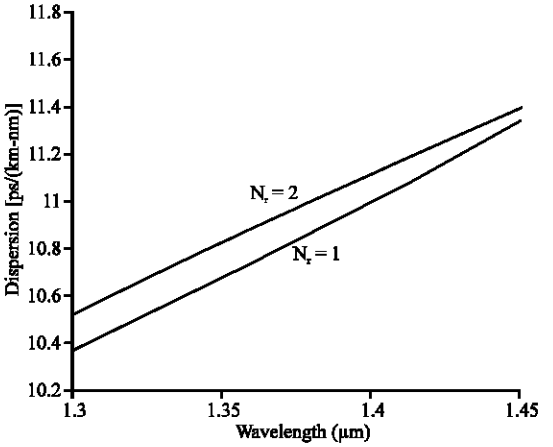

Fig. 7: Dispersion of photonic crystal fiber against wavelength for different number of air hole rings. Air hole diameter, d = 6 μm and hole spacing, Λ = 6.75 μm.

PCF exhibits a very large effective mode area. It is found that the effective mode area decreases with the increased number of air hole rings.

Figure 5-7 depict the dispersion property of photonic crystal fiber against wavelength for different structural parameters. In each case it is found that the dispersion increases with the increase of operating wavelength, which agrees with the results found in Saitoh and Koshiba (2003) and Tajima *et al.* (2004) and the amount of increment is small compared to that of the conventional optical fiber, resulting almost flattened

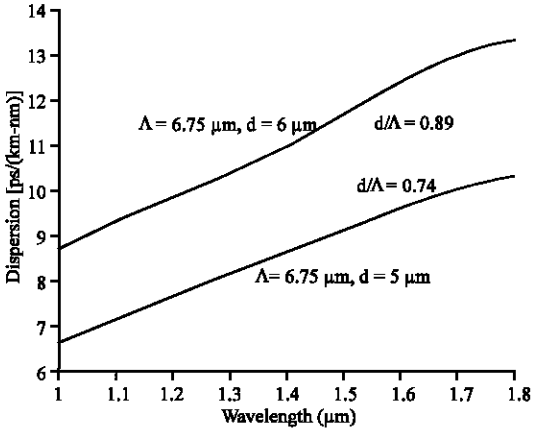

Fig. 8: Dispersion of photonic crystal fiber against wavelength for different air hole diameter. Air hole spacing, Λ and number of air hole rings, N_r is constant

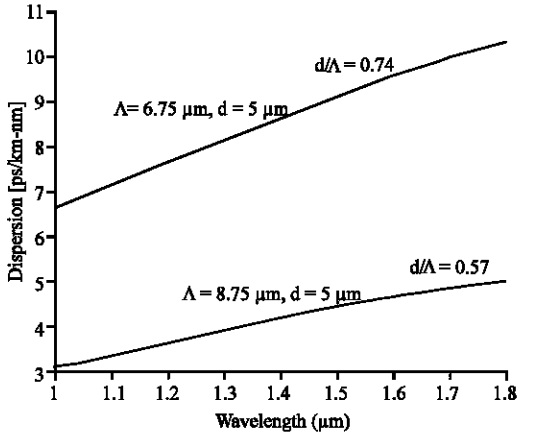

Fig. 9: Dispersion of photonic crystal fiber against wavelength for different air hole spacing. Air hole diameter, d and number of air hole rings, N_r is constant

dispersion profile. It is also found, that the dispersion increases with the increasing number of air hole rings.

Figure 8 depicts the dispersion property of photonic crystal fibers against wavelength for different air hole diameters. It is found that the dispersion increases with the increase in air hole diameter that agrees with the results found in (Shen *et al.*, 2003).

Figure 9 depicts the dispersion property of photonic crystal fiber against wavelength for different pitch. It is found that the dispersion decreases with the increase in pitch.

Figure 10-12 depict confinement loss as a function of wavelength for different structural parameters. In each

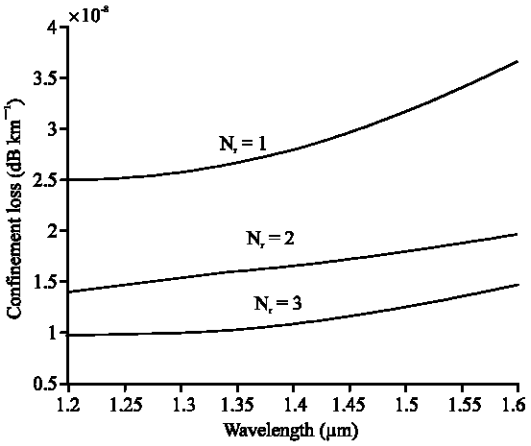

Fig. 10: Confinement loss of photonic crystal fiber against wavelength for different number of air hole rings. Air hole diameter, d = 5 μm and pitch Λ = 6.75 μm

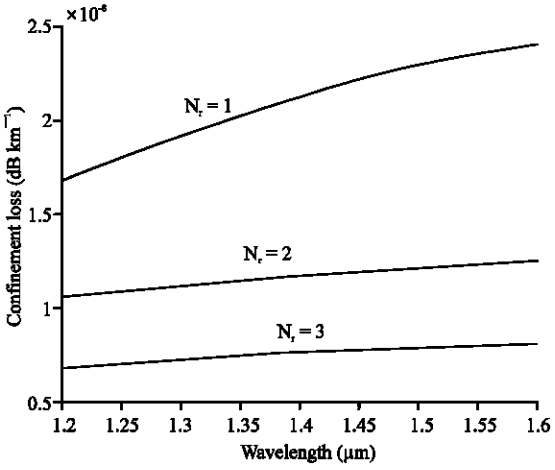

Fig. 11: Confinement loss of photonic crystal fiber against wavelength for different Number of air hole rings. Air hole diameter, d = 5 μm and pitch Λ = 8.75 μm

case it is found that confinement loss decreases with the increase in number of air hole rings that agrees with the result found in (Finazzi *et al*., 2003).

Figure 13 and 14 show the confinement loss as a function of wavelength for different air hole spacing and for different air hole diameter, respectively. It is found that the confinement loss decreases with the increase in pitch of the fiber that agrees with the result found in (Finazzi *et al*., 2003). It is also, found that the confinement loss increases with the increase of air hole diameter.

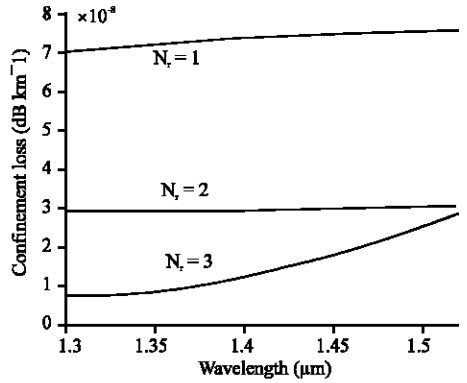

Fig. 12: Confinement loss of photonic crystal fiber against wavelength for different Number of air hole rings. d = 6 μm and Λ = 6.75 μm

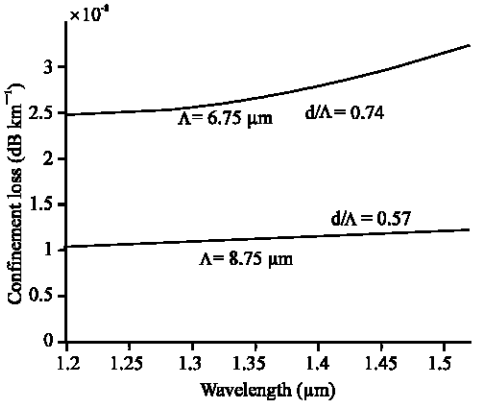

Fig. 13: Confinement loss of photonic crystal fiber against wavelength for different air hole pitch. Air hole diameter, d and number of air hole rings, N_r is constant

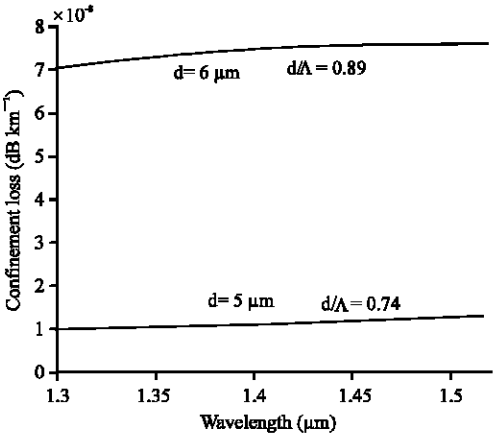

Fig. 14: Confinement loss of photonic crystal fiber against wavelength for different air hole diameter. Air hole pitch, Λ and number of air hole rings, N_r is constant

CONCLUSION

An efficient approach of the finite element method in the FEMLAB environment is used for the analysis of PCF. It has been found that the effective mode index decreases with the increase of wavelength and air hole diameter and increases with the increase of pitch of PCF. It has been observed that the electric field distribution becomes more concentrated to the centre when the number of air hole rings is increased. The effective modal area of the PCF has been found to be large compared to that of the conventional optical fiber and it decreases with the increase in number of air hole rings. Dispersion and confinement loss are calculated for different structural parameters. It has been found that dispersion increases with the increase in wavelength, number of air hole rings and air hole diameter, respectively and that decreases with the increase in pitch length. It is also found, that confinement loss decreases with an increase in number of air hole rings and air hole spacing and that increases with the increase in air hole diameter. The results will find application, in designing of a photonic crystal fiber for a particular effective mode area, dispersion and confinement loss.

REFERENCES

Alam, M.S., K. Saitoh and M. Koshiba, 2005. High group birefringence in air-core photonic crystal fibers. Opt. Lett., 30 (8): 824-826.

Birks, T.A., J.C. Knight and P. Russel, 1997. Endlessly single mode photonic crystal fiber. Opt. Lett., 22 (13): 961-963.

Ferrando, A., E. Silvestre, J.J. Miret and P. Andres, 1999. Full vector analysis of realistic photonic crystal fiber. Opt. Lett., 24 (5): 276-278.

Finazzi, V., T.M. Monro and D.J. Riharson, 2003. Small-core silica holey fibers: nonlinearity and confinement loss trade-offs. J. Opt. Soc. Am. B, 20 (7): 1427-1436.

Knight, J.C., 2003. Photonic crystal fibers. Nature, 424: 847-851.

Knight, J., T. Birks, R. Cregon, P. Russel and J. Sandro, 1998. Large mode area photonic crystal fiber. Electron. Lett., 34 (13): 1347-1348.

Matsui, T., J. Zhou, K. Nakajima and I. Sankawa, 2005. Dispersion flattened photonic crystal fiber with large effective area and low confinement loss. J. Lightwave Technol., 23 (12): 4178-4183.

Russel, P., 2003. Photonic crystal fibers. Science, 299: 358-362.

Saitoh, K. and M. Koshiba, 2003. Chromatic dispersion control in photonic crystal fibers: Application to ultra-flattened dispersion. Opt. Express, 11 (8): 843-852.

Shen, L., W. Huang and S. Jian, 2003. Design of photonic crystal fibers for dispersion related applications. J. Lightwave Technol., 21 (7): 1644-1651.

Tajima, K., J. Zhou, K. Nakajima and K. Sato, 2004. Ultralow loss and long length photonic crystal fiber. J. Lightwave Technol., 22 (1): 7-10.

White, T.P., B.T. Kuhlmey, R.C. McPhedran, D. Maystre, G. Renversez, C.M. Sterke and L.C. Botten, 2002. Multipole method for microstructured optical fibers. J. Opt. Soc. Am. B, 19 (10): 2322-2330.

Zolla, F., G. Reneversez, A. Nicolet, B. Kuhlmey, S. Guenneau and D. Felbacq, 2005. Foundation of Photonic Crystal Fibers. 1st Edn. Imperial College Press.